Multistep relaxation in equilibrium polymer solutions: A minimal model of relaxation in "complex" fluids

Evgeny B. Stukalin,[1,a)] Jack F. Douglas,[2] and Karl F. Freed[1]
[1]*The James Franck Institute, University of Chicago, Chicago, Illinois 60637, USA*
[2]*Polymers Division, National Institute of Standards and Technology, Gaithersburg, Maryland 20899, USA*

(Received 3 March 2008; accepted 5 August 2008; published online 5 September 2008)

We examine the rheological and dielectric properties of solutions of equilibrium self-assembling particles and molecules that form polydisperse chains whose average length depends on temperature and concentration (free association model). Relaxation of the self-assembling clusters proceeds by motions associated either with cluster rotations, with diffusive internal chain dynamics, or with interchain entanglement interactions. A hierarchy of models is used to emphasize different physical effects: Unentangled rodlike clusters, unentangled flexible polymers, and entangled chains. All models yield a multistep relaxation for low polymer scission rates ("persistent polymers"). The short time relaxation is nearly exponential and is dominated by the monomeric species and solvent, and the long time relaxation is approximately a stretched exponential, $\exp[-(t/\tau)^{\beta}]$, a behavior that arises from an averaging over the equilibrium chain length distribution and the internal relaxation modes of the assembled structures. Relaxation functions indicate a *bifurcation* of the relaxation function into fast and slow contributions upon passing through the polymerization transition. The apparent activation energy for the long time relaxation becomes temperature dependent, while the fast monomeric relaxation process remains Arrhenius. The effective exponent $\beta(T)$, describing the long time relaxation process, varies monotonically from near unity above the polymerization temperature to a low temperature limit, $\beta \simeq \frac{1}{3}$, when the self-assembly process is complete. The variation in the relaxation function with temperature is represented as a function of molecular parameters, such as the average chain length, friction coefficient, solvent viscosity, and the reaction rates for particle association and dissociation. © *2008 American Institute of Physics*.
[DOI: 10.1063/1.2976341]

I. INTRODUCTION

The nontrivial correlations created by the transient formation and disintegration of particle clusters in complex fluids can induce significant changes in their transport properties whose theoretical description is basic in understanding the dynamics of numerous "associating fluids" (micellar fluids,[1] equilibrium polymers,[2] thermally reversible gels,[3] and glass-forming liquids[4–6]). Such fluids are characterized by dynamic heterogeneity, even though these complex fluids may differ considerably in the physical interactions driving dynamic clustering. The macroscopic viscoelastic and dielectric properties of these fluids appear to exhibit a common pattern of relaxation that includes the (a) emergence of fast and slow relaxation processes separated by an intermediate plateau in the stress relaxation, (b) a stretched exponential (SE) relaxation, (c) a non-Arrhenius dependence of the structural relaxation time, etc.[7–9]

In the present paper, we consider a minimal model of relaxation involving the equilibrium self-assembly of molecules and particles into polymer chains that form and disintegrate in dynamic equilibrium. This minimal model is formulated in terms of microscopic properties (molecular friction coefficients and interaction parameters) describing the clustering and is found to exhibit the general pattern of relaxation in the complex fluids mentioned earlier. In particular, the stress relaxation, viscosity, and dielectric relaxation functions for equilibrium self-assembling systems are computed using classic rodlike chain, Rouse, and reptation models of chain dynamics. A previous paper introduced much of the required theoretical framework,[10] and the present work focuses on the wide range of implications of the theory. While the treatment below is restricted to systems in which self-assembly occurs upon cooling, the theory is also applicable to cases where association proceeds on heating. Our modeling of relaxation in associating fluids omits the hydrodynamic interactions that lead to nonexponential relaxation (i.e., "memory" effects) even in simple fluids. Hydrodynamic interactions are often ignored when phenomenologically modeling polymer fluids, especially at high polymer concentrations where the hydrodynamic interactions become screened.[11] (See Sec. IV.) We also do not include memory effects associated with strong local interparticle interactions or "caging" interactions that are emphasized by the mode-coupling theory of glass-forming liquids[12,13] and its recent generalization.[14] Despite these assumptions, we believe that our model provides basic insight into the multistep relaxation observed in many complex fluids in which "dynamic heterogeneity" (i.e., dynamic particle clustering) is involved. This expectation remains to be confirmed, however.

Above the polymerization temperature where self-

a)Electronic mail: stukalin@uchicago.edu.

assembly initiates, only exponential stress relaxation is found, but an additional slow relaxation process emerges at lower temperatures where persistent chain clusters are present. The terminal relaxation time τ_T, associated with this slow relaxation mode, becomes increasingly prominent upon cooling, and the relaxation function for this mode is found to be approximately a SE, $G(t) \sim \exp[-(t/\tau)^{\beta}]$, with β varying monotonically from unity at high temperatures to a constant at lower temperatures where the clustering transition is fully developed. The low temperature limiting β for persistent rodlike associating clusters and for persistent polymer chains exhibiting reptation dynamics is found universally to be near $\beta=\frac{1}{3}$, in accord with the single mode approximation of Douglas and Hubbard (see below).[15]

The averaging over the internal modes of flexible self-assembled chains is shown to influence the effective β, reducing its value at lower temperatures. The computed pattern of multistep relaxation and long time SE decay predicted by our theory appears to be similar to the general pattern seen in many complex associating fluids, although the thermodynamic variables governing the clustering (chain length, added salt, concentration, temperature, pressure, etc.) and the geometrical form of the clusters (linear and branched chains, membranes, compact clusters) vary between these systems. While the actual geometry of the clusters may vary with the particular associating fluid, giving rise to a change in the exponent β at low temperatures,[15] we expect the pattern of relaxation that we find for linear chain association to apply generally to complex fluids in which assembly into highly extended structures occurs.

The equilibrium self-associating fluid model for stress and dielectric relaxations is rather complicated computationally, so essential features of this model are illustrated for representative model parameters. The first model considers equilibrium clusters that form rodlike structures under conditions where interchain excluded volume interactions are absent.[16,17] Although this model lacks internal chain modes, the chain length polydispersity and the tunable average chain length produce nontrivial viscoelastic and dielectric responses. The second model involves ideally flexible (random walk) chains where the internal mode dynamics is described using the mean-field Rouse theory, which neglects interchain hydrodynamic interactions.[18–20] This model illustrates how the internal modes of the chains and chain polydispersity affect the viscoelasticity of the self-assembling fluid. Finally, we consider a mean-field model of chains with appreciable interchain excluded volume interactions (reptation model) to provide insight[18] into how the contribution of interchain interactions influence relaxation in complex fluids where "entanglement" interactions are prevalent.

Section II briefly summarizes essential definitions of equilibrium polymerization models and the basic variables of the theory. The general theory is then applied to the following systems: The reversible formation of rodlike polymers, flexible polymers (Rouse model), and chains with strong intermolecular chain interactions (reptation model). Moments S_j of the stress relaxation function $G(t)$ are used to quantify the broadening of stress relaxation induced by the wide polydispersity of the equilibrium clusters. Section III describes applications of the theory to dielectric relaxation from calculations of the autocorrelation function $\psi(t)$ for the end-to-end vector, and we contrast the variation in $\psi(t)$ with that in $G(t)$. The Appendix discusses the alternative two-parameter Cole–Davidson (CD) representation of relaxation phenomena, and interrelations are established between the SE and CD parameters that approximately describe relaxation in associating fluids.

II. STRESS RELAXATION IN EQUILIBRIUM POLYMERS

Consider a self-assembling solution in which the chain length distribution is determined by a reaction equilibrium and by the overall concentration ϕ of the solute. The simplest model is the "freely associating" (FA) model in which all solute species are permitted to associate and disintegrate without constraint.[21] This minimal model is consistent with at least two alternative reaction mechanisms.[10] The first is the monomer-mediated (MM) model[22] described as,

$$A_N \rightleftharpoons A_{N-1} + A_1, \quad \text{MM model}, \tag{1}$$

while the other is the scission-recombination (SR) scheme,[1]

$$A_N \rightleftharpoons A_{N'} + A_{N''}, \quad \text{SR model}, \tag{2}$$

where $N=N'+N''$. Each association and dissociation event involves the formation or breaking of a single "bond" in the linear chain clusters, and k_a and k_d are the mean-field rate constants for chain growth and scission, respectively. Both rate constants are assumed, for simplicity, to be independent of chain length and configuration. The SR and MM reaction kinetics both yield the same equilibrium chain distributions for the FA polymer system,

$$c_N = \phi L^{-2} q^{N-1} \simeq \phi L^{-2} \exp(-N/L), \tag{3}$$

where c_N is the number density of chains with length N, ϕ is the total monomer density satisfying $\phi=\Sigma_N N c_N$,[22] and $q=1-1/L<1$, with L the average chain length. L depends on the equilibrium constant $K_{\mathrm{eq}}=k_a/k_d$ for the addition of a monomer and on the initial concentration ϕ,

$$L = \frac{2\phi K_{\mathrm{eq}}}{\sqrt{1+4\phi K_{\mathrm{eq}}}-1} \simeq \phi^{1/2} \exp(-\Delta s/2k_B)\exp(\Delta h/2k_B T), \tag{4}$$

where Δh and Δs are energy and entropy changes for chain scission, and the mean-field rate constants k_d and k_a are assumed to have an Arrhenius temperature dependence,

$$k_d = \delta_d \exp[-\varepsilon_d/k_B T], \qquad k_a = \delta_a \exp[-(\varepsilon_d - \Delta h)/k_B T], \tag{5}$$

where ε_d is the activation energy for the scission reaction. When N is treated as a continuous parameter, the equilibrium number density likewise also emerges as the exponential distribution of Eq. (3) (which applies for $L \gg 1$).[23,24]

The influence of particle clustering is illustrated by comparing the behavior of polydisperse systems of "frozen," nonassociating chains with solutions of "dynamic" or "living" chains where each system has the same exponential

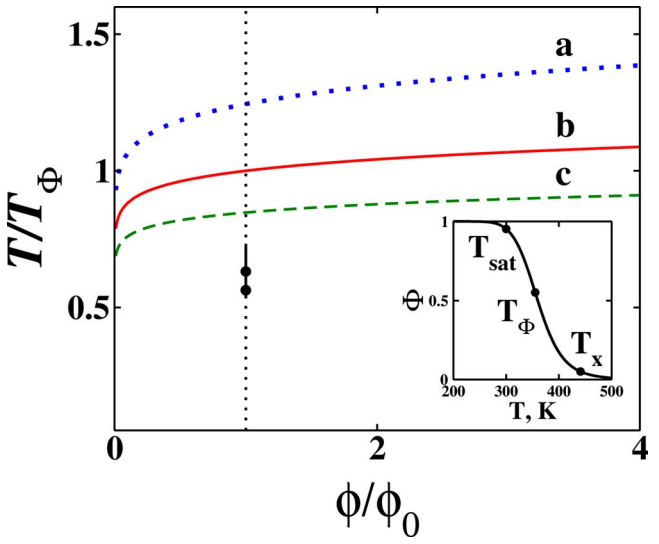

FIG. 1. (Color online) Concentration dependence of characteristic polymerization temperatures: (a) "Onset" T_x, (b) inflection point T_Φ, and (c) "saturation" T_{sat} temperatures for the quasichemical free association model of equilibrium self-assembly. $T_\Phi = 355$ K is the "polymerization" temperature for the solution having a reference concentration ϕ_0. The two filled circles correspond to the states chosen in Fig. 2, and the solid line denotes the cooling history for obtaining β in Figs. 3 and 6. The dotted line passes through the polymerization transition. The inset depicts the degree of association Φ as a function of temperature.

chain length distribution as Eq. (3). The description of the temperature dependence of viscoelastic properties is facilitated by defining the polymerization temperature T_Φ as the inflection point in the temperature dependence of the fraction $\Phi(T)$ of monomers in the clusters,

$$\frac{d^2\Phi(T)}{dT^2} = \frac{d^2}{dT^2}\left(1 - \frac{1}{L^2(T)}\right) = 0. \tag{6}$$

The polymerization temperature can be also defined as the temperature where the specific heat capacity $C_v(T)$ of the system is maximum[25] or alternatively as the "kink" in the mass density for a compressible fluid.[26] The onset of association upon cooling occurs at a temperature T_x, the monomers are largely consumed at a temperature T_{sat}, and T_Φ is an intermediate temperature (see Fig. 9 of Dudowicz *et al.*[25] and the related discussion). The locus of onset T_x and saturation T_{sat} temperatures (see inset of Fig. 1) are calculated for the quasichemical FA model as the characteristic temperatures where the degree of polymerization approaches $\Phi(T_x) = 0.05$ and $\Phi(T_{sat}) = 0.95$, respectively.[21,25] These characteristic temperatures vary monotonically with the initial monomer concentration, and their loci provide the "state diagrams" (the analog of phase boundaries in phase separating or crystallizing systems) for this and many other self-assembling systems in solution (see Fig. 1). Note that $\phi v_{A_1} = \phi_1^0$, where ϕ_1^0 denotes the initial volume fraction of monomers[25] and v_{A_1} is the volume of a monomer subunit.

The stress relaxation modulus $G(t)$ for an equilibrium associating fluid involves contributions from both the self-assembled species and the unassociated monomeric particles. To minimize the number of parameters, the subunits are taken to have identical relaxation behavior as the solvent particles. Since the relaxation of the solvent and monomers is not described by either of the classical polymer models, their contribution to the short time stress relaxation is described using the simplest Maxwell model, while the long time contribution from chain dynamics is treated separately, as illustrated below using the simple Rouse, reptation, and rodlike chain dynamical models with modifications introduced to describe the reversible scission/association processes.

The evaluation of the contribution to the stress relaxation function $G(t)$ from the clusters requires summing over the normal modes for the collective chain motions and then averaging over the equilibrium size distribution (q^{N-1} in the simple FA model),[10]

$$G(t) \simeq G_\infty \exp(-t/\tau_m) + \frac{1}{L^2}\sum_{N=2}^{+\infty}\sum_{p=1}^{N-1} G_{0,N} N q^{N-1} \sigma(p) \times \exp(-t/\tau_p)\exp(-t/\tau_d), \tag{7}$$

where τ_d is the characteristic time for reaction (1) or reaction (2), whose dependence on N is given explicitly in Eq. (9) below, while τ_p are the normal mode relaxation times of the linear chains. A similar scheme for describing relaxation in equilibrium polymers by a weighted average as in Eq. (7) has been introduced by Faivre and Gardissat[27] and also by Huang *et al.*[28] $G_{0,N}$ is the "plateau modulus" for clusters with fixed length N, while $G_\infty = G_s^0 + (1-\Phi)G_m^0$ accounts for the contributions from solvent and monomer particles, respectively. The relaxation times $\tau_m = \tau_m^0 \exp(\varepsilon_s/k_BT)$ for the solvent and monomers are set equal for simplicity, but this assumption is not required. Equation (7) recognizes that the monomer contribution at lower temperatures is proportional to the concentration of the unassociated monomers which become depleted as the monomers join into chains, while at high temperatures the relaxation of the unassociated species dominates. The mode dependent factor $\sigma(p)$ is specific to the polymer model (stiff chains, flexible chains, rods, etc.) and is thus a dynamical quantity to be computed. For instance, our computations of the relaxation modulus $G(t)$ for the Rouse model of associating polymers indicate that $\tau_p \simeq \tau_0 N^2/p^2$ and $\sigma(p) = 1$, while the treatment of dielectric relaxation with the Rouse model of associating polymers involves the normalized time correlation function for the end-to-end vector $\psi(t) = \langle R(t)R(0)\rangle/\langle R^2\rangle$, a description that requires the summation over odd modes with the factor $\sigma(p) = 1/p^2$,

$$\psi_N(t) = \frac{8}{\pi^2}\sum_{p=1}^{N-1}\frac{1}{p^2}\exp(-t/\tau_p)\exp(-t/\tau_c) \quad (p \text{ odd}). \tag{8}$$

Likewise, the contribution to the stress relaxation from chains with fixed length N undergoing *reptation* dynamics is proportional to $\psi_N(t)$ of Eq. (8) with $\tau_p = \tau_{\mathrm{rep},N}/p^2$, $\tau_{\mathrm{rep},N} = \tau_{\mathrm{rep}}(N/L)^3$, and $\sigma(p) = 1/p^2$. The "single mode approximation" involves simply restricting the sums in Eqs. (7) and (8) to $p = 1$.

Finally, the characteristic times for the scission/association reactions are taken as the average lifetimes τ_d of the linear chain clusters, which are obtained in Ref. 10 as

$$\tau_d = \begin{cases} \dfrac{1}{2k_d} & \text{for MM reaction} \\ \dfrac{1}{k_d(2L+N)} & \text{for SR reaction.} \end{cases} \tag{9}$$

These equations assume that chain scission is unimolecular and arises either at the chain ends (MM) or occurs with uniform rate along the chain (SR). Thus, the temperature dependence of the chain scission time is governed by the variations in the dissociation rate constant k_d and the average chain length L. For instance, the average chain scission time for SR kinetics changes as $\tau_d \simeq (k_d L)^{-1} \sim \exp(\varepsilon_d / k_B T)\exp(-\Delta h / 2k_B T)$.

Stress relaxation in equilibrium self-associating fluids becomes particularly simple at high temperatures (clustering upon cooling) when τ_d is less than the time $\tau_D = D\langle R^2\rangle/6$ for ideally unbreakable chains to diffuse a distance on the order of the mean square end-to-end distance $\langle R^2\rangle$, where D is the average diffusion coefficient of the unbreakable chains. The low temperature limit of $G(t)$ in Eq. (7) then reduces to a simple exponential relaxation, the classic Maxwell viscoelastic relaxation model.[17] (This result applies to the rodlike chain, the flexible chain, and even the reptation model and thus is quite general.) The later nontrivial case was first noted by Cates[29] in pioneering modeling of the dynamics of wormlike polymers. Numerous experiments for aqueous surfactants forming wormlike micelles and other systems forming equilibrium associates seem to conform remarkably well to this simple exponential relaxation.[30–32]

Unsurprisingly, the Maxwell relaxation is not universally observed, which has led to some questioning of validity of the model of Cates.[29] In our view, this judgment is premature, and we focus instead on the obvious possibility that experimental deviations from the Maxwell model may be explained in terms of the more general Eq. (7) where the relaxation process involves a complicated interplay between fission, chain diffusion, influence of interchain interactions, and relaxation modes of the self-assembled chains. Since our goal is not to specifically model aqueous wormlike micelles or chain forming gelator molecules in organic solvents,[34] the models treated here are not designed specifically for describing these particular associating fluids. The focus, instead, is on general phenomena describing how chain polydispersity under equilibrium conditions, chain flexibility, and interchain excluded volume interactions affect the stress relaxation in solutions of equilibrium clusters for conditions ranging from partially persistent chains ($\tau_d \simeq \tau_D$) to highly persistent chains ($\tau_d \gg \tau_D$). The results below demonstrate that stress and dielectric relaxation can exhibit a much more complicated relaxation than that predicted by the Maxwell model when the self-assembled chains are persistent, thereby acting more like conventional polymer solutions where the bonds mimic essentially irreversible chemical reactions. Many of our results qualitatively agree with the observed nonexponential stress relaxation for associating fluids with persistent chains,[31,34–37] while Turner and Cates[38] and Granek and Cates[39] described the effect of chain persistence using the SR-FA model of equilibrium association and reptation.

Measurements of the compliance provide valuable information concerning stress relaxation in self-assembling solutions. The equilibrium steady-state compliance[17] J_e probes the relation between the $n=1$ and $n=2$ moments $\langle\Lambda^n\rangle$ of the relaxation time distribution for the system,

$$J_e = \int_0^\infty tG(t)dt \Big/ \left[\int_0^\infty G(t)dt\right]^2 = \lim_{\omega\to 0}\frac{G'(\omega)}{G''(\omega)^2} \equiv G_0^{-1}\langle\Lambda^2\rangle/\langle\Lambda\rangle^2. \tag{10}$$

The analysis of J_e for various models of reversibly associating systems is most conveniently executed using the last equality of Eq. (10) in conjunction with the SE model as represented in the frequency domain. The imaginary Laplace transform $\mu^*(\tau\omega,\beta)$ of the SE is well approximated for low frequencies by the first two terms of the series in Eq. (A4) of the Appendix,

$$\mu^*(\tau\omega,\beta) \simeq \frac{1}{\beta}[\Gamma(1/\beta)i\tau\omega + \Gamma(2/\beta)\tau^2\omega^2], \tag{11}$$

which is used below to analyze our calculations for models of the dynamics of equilibrium associating systems, such as the scission-Rouse or scission-reptation models. More specifically, the steady-state compliance J_e computed with these models using Eq. (10) is equated with its analog from the SE model from Eq. (11),

$$J_e G_0 = \frac{\langle\Lambda^2\rangle}{\langle\Lambda\rangle^2} = \frac{\beta\Gamma(2/\beta)}{\Gamma^2(1/\beta)}, \tag{12}$$

enabling the determination of the model and system dependent parameter $\beta \le 1$ that optimally fits the low frequency portion of $G^*(\omega)$. The product $J_e G_0$ provides a useful measure of the breadth of the stress relaxation process.

A. Rodlike model for equilibrium polymers

The single mode approximation is most accurate for the relaxation of an equilibrium mixture of straight cylindrical macromolecules. The theory of frozen, monodisperse rodlike clusters predicts the frequency dependency of the dynamic shear moduli as[17]

$$G'(\omega) = \frac{G_0}{N}\frac{m_1\omega^2\tau_{\mathrm{rod},N}^2}{1+\omega^2\tau_{\mathrm{rod},N}^2}, \qquad G''(\omega) = \frac{G_0}{N}\left(\frac{m_1\omega\tau_{\mathrm{rod},N}}{1+\omega^2\tau_{\mathrm{rod},N}^2} + m_2\omega\tau_{\mathrm{rod},N}\right), \tag{13}$$

where $G_0 = \rho RT/M_0 = \phi k_B T$, M_0 is the molecular mass of a monomer, ρ is the cluster mass concentration which is related to the total monomer density ϕ in solution by $\rho = \phi M_0/N_A$ (N_A is the Avogadro number), the rotational relaxation time $\tau_{\mathrm{rod},N}$ of the cylinder equals

$$\tau_{\mathrm{rod},N} = \frac{\pi\eta_s N^3 F(N/d)}{18k_B T} \simeq \tau_s N^3, \tag{14}$$

m_j are model specific constants ($m_1 = \frac{3}{5}$ and $m_2 = \frac{1}{5}$; see Ref. 17), F is a slowly varying function of N/d that is of order

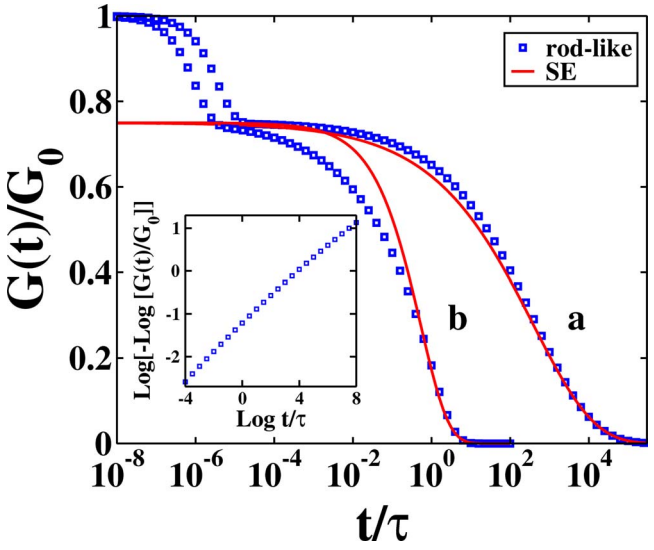

FIG. 2. (Color online) Multistep stress relaxation function for polydisperse mixtures (a) of unbreakable rodlike clusters with average length $L=600$ and $\tau_s=3.8\times10^{-6}$ at a low temperature $T/T_\Phi=0.563$ and (b) of living rods with average length $L=120$ and $\tau_s=1.0\times10^{-6}$ at a higher temperature $T/T_\Phi=0.631$ (open squares). $\tau_{\mathrm{rod}N}\simeq\tau_sN^3$ is the rotational relaxation time of monodisperse rods at fixed N. The short time relaxation constant is $\tau_m=\tau_s$, and the ratio $G_\infty:G_{0,L}$ is taken as 1:3. The solid lines are SE fits with (a) $\beta=0.28$ and (b) $\beta=0.62$, respectively, to the long time portion of the relaxation function as deduced from the steady-state compliance J_eG_0 for the same temperatures. The inset depicts the long time contribution to $G(t)$ for the rodlike model of unbreakable rods at $T/T_\Phi=0.563$. The model parameters used are $\Delta h=20k_BT_0$, $\varepsilon_m=\varepsilon_s=8k_BT_0$, and $\varepsilon_d=115k_BT_0$ ($T_0=300$ K). The polymerization temperature T_Φ is determined from the inflection point of $\Phi(T)$ as $T_\Phi=355$ K.

unity, d is the diameter of the stiff cylindrical macromolecule, N is its length, and τ_s is a segmental relaxation time,

$$\tau_s \simeq \tau_s^0 \exp(\varepsilon_s/k_BT). \tag{15}$$

The near proportionality of $\tau_{\mathrm{rod},N}$ to N^3 is similar to the scaling of the reptation time $\tau_{\mathrm{rep},N}$.[18] Thus, the computations of $G(t)$ from Eq. (7) with $\sigma(p)=\delta_{1p}$ involve the single mode relaxation time $\tau_p=\tau_{\mathrm{rod},N}$ for the rodlike cluster with length N from Eqs. (14) and (15). For consistency, the long time contribution in Eq. (7) to the $N=1$ "one bead" limit is required to reproduce the short time contribution (taken separately) at high temperatures above the polymerization temperature. This consistency condition introduces interrelations between parameters, namely, the zero-shear viscosity $\eta_0(T_x)$ of the solution of unassociated single beads at high temperatures is chosen to equal to that computed using the Maxwell model describing the contribution from "monomers." This condition implies $\eta_0(T_x)=G_m^0\tau_m\simeq G_0\tau_s$. The modulus ratio G_s^0/G_m^0 is best obtained from experiment and is treated as a parameter below.

Figure 2 displays the stress relaxation modulus of a FA equilibrium mixture for persistent, unbreakable rodlike clusters at low temperatures $T\ll T_\Phi$, where SR or MM reaction kinetics are too slow to influence cluster relaxation, and also at higher temperatures where the scission rates impact significantly the relaxation dynamics of the rods formed by dynamic association. The illustrative parameters are indicated in the caption. Remarkably, $G(t)$ exhibits a nearly flat plateau for $\tau_m<t<\tau_{\mathrm{rod},L}$. The width of the plateau grows with diminishing temperature as the average chain length L increases. This behavior occurs because the relaxation times τ_{rod} for linear chain clusters are proportional to τ_sN^3, and the height of the plateau generally also depends on L because the height is governed by the ratio G_0/G_∞. Above the polymerization temperature $T>T_\Phi$, long chains dissociate into monomers, so the high temperature system exhibits the short time relaxation of the monomer-solvent mixture (presumed here to be an exponential relaxation). A plateau in $G(t)$ develops at lower temperatures when the ratio of characteristic relaxation times $\tau_{\mathrm{rod},L}/\tau_m$ becomes large. Consequently, the height of the plateau decreases with cooling as the fraction of monomers diminishes. The long time decay of $G(t)$ is dominated by the relaxation modes of the linear chain clusters with the length distribution dictated by the equilibrium FA model. The multistep decay of Fig. 2 is qualitatively similar to data from the dynamic light scattering autocorrelation function and corresponding stress relaxation data (which have a more limited accessible time range) for persistent or "entangled" wormlike micelle solutions.[37]

The long time relaxation process obtained from Eq. (7) is well represented by a SE, as demonstrated in Fig. 2. The exponent $\beta\simeq0.30$ agrees well with the time variation in $G(t)$ over many decades at low temperatures, i.e., for the corresponding frozen polydisperse system. This finding is encouraging in view of data for the rheology of wormlike micelles where the apparent β for aqueous cetylpyridinium chloride surfactant with added Na-salicylate salt (293 K) varies from a low limit near 0.3 to almost 1.0 as the salt concentration increases relative to that of the surfactant.[32]

An alternative approximation for β may be evaluated from the equilibrium steady-state compliance J_e using Eq. (10), so both methods of evaluating β are compared. Disregarding the purely viscous (m_2) contribution to G'' in Eq. (13) for the relaxation function of unbreakable, polydisperse rods ($k_d\to0$), the low frequency limit of the complex modulus $G^*(\omega)$, normalized by $g_0\equiv G'(\omega\gg0)=G_0/(Lm_1)$, yields

$$G'(\omega)/g_0 \simeq 720\tau_s^2L^6\omega^2,$$
$$G''(\omega)/g_0 \simeq 6\tau_sL^3\omega, \tag{16}$$

where L is the average length of the frozen chains.

The computed compliance $J_eg_0\simeq20.0$ for the polydispere mixture of unbreakable rodlike molecules and the use of Eq. (12) yield $\beta\simeq0.28$, which agrees well with the exponent $\beta\simeq0.30$ obtained by fitting the long time portion of the computed $G(t)$ in the time domain. Below we demonstrate that all three models (Rouse, rodlike, and reptation) for frozen chains with an exponential length distribution produce similar SE long time behaviors with the *quasiuniversal* exponent $\beta\simeq\frac{1}{3}$, as predicted by Douglas and Hubbard[15] within the single mode approximation.

When the scission rates of the rodlike molecules are non-negligible, the apparent stretched exponent deduced from fitting the long time portion of $G(t)$ can exceed $\frac{1}{3}$. Indeed, the average of the normalized long time contribution from Eq. (7) translates in the frequency domain for small ω to the relations

$$G'(\omega)/g_0 \simeq L\tau_s^2\omega^2\bar{S}_2,$$
$$G''(\omega)/g_0 \simeq L\tau_s\omega\bar{S}_1, \tag{17}$$

where the moments $\bar{S}_j(j=1,2)$ of the cluster size distribution can be evaluated analytically using a continuous chain length distribution instead of a discrete summation as

$$\bar{S}_j = \frac{1}{L^2}\int_0^\infty \frac{N^{3j}}{(1+r)^j}\exp(-N/L)dN, \tag{18}$$

and where the dimensionless parameter r in Eq. (18) is defined by

$$r \equiv \begin{cases} 2\tau_s N^3 k_d & \text{for MM kinetics} \\ \tau_s N^3 k_d(2L+N) & \text{for SR kinetics.} \end{cases} \tag{19}$$

The frozen system (of infinitely persistent chains) corresponds to $k_d=0$ and, consequently, to the limit $r=0$, so that Eq. (17) transforms to Eq. (16) describing the case of frozen rods. Comparing Eqs. (17) and (11) enables evaluation of the stretching parameters relevant to the low frequency domain for reversible systems where $r>0$. When the reaction kinetics are relatively rapid ($r \gg 1$), the coefficients from Eq. (18) become $L\bar{S}_2 \simeq (L\bar{S}_1)^2 \simeq$ const, and Eq. (12) implies that the relaxation function is exponential at long times with $\beta \simeq 1$.

It is interesting to consider how the computed β from $G^*(\omega)$ at small ω compares with that obtained from fitting the relaxation function $G(t)$ at long times. Our analysis indicates that the apparent β evaluated from the computed $G(t)$ changes systematically with the range of time used in the fitting process. Clearly, at sufficiently short times, scission events do not affect the relaxation process, while at very long times the dominant contributions to $G(t)$ are provided by the longest rods, whose "efficiencies" of chain relaxation $\tau_{\mathrm{rod},N}/\tau_c$ are amplified by their nonzero scission rates. Hence, $\beta \simeq 1$ is also expected to emerge from $G(t)$ in the limit of extremely long times, but this situation is only of academic interest since $G(t)$ has essentially decayed to zero at such long times. The intermediate time domain yields an apparent stretching exponent β that changes smoothly between these two regimes for equilibrium associating systems. The apparent β from fits to the low frequency portion of $G^*(\omega)$ for associating solutions of rodlike macromolecules corresponds to that computed for $G(t)$ in the "intermediate" time range for the relaxation of rods with average length L whose range of effective relaxation times overlaps the time domain used in the fitting process.

The apparent exponent β naturally depends on temperature because of the variation in the cluster size distribution, reaction rates, and rates of cluster diffusive rearrangements, implying more specifically the change in the average chain length L, rate constant k_d, and structural relaxation times, i.e., τ_{rod}) with temperature. Below, we briefly illustrate how β varies from a low β plateau regime for persistent rodlike chains at low temperatures $T \ll T_\Phi(r \simeq 0)$ to $\beta \simeq 1$ for the short lived species characterized by appreciable scission rates at higher temperatures $T > T_x(r \geq 1)$. The dissociation constant k_d in systems self-assembling on cooling increases

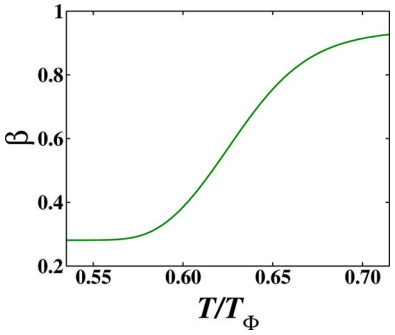

FIG. 3. (Color online) The sigmoidal temperature dependence of the fits of β to the low frequency portion of $G^*(\omega)$ for the scission-rodlike model of dynamics and aggregation. The model parameters for the scission and activation energies are the same as in Fig. 2.

with temperature, while the average chain length L decreases. When the SR mechanism is operative, both factors produce a change in β as we detail below.

The temperature dependence of the time scale for chain diffusive rearrangements in Eqs. (14) and (15) and for scission of the clusters in Eqs. (5) and (9) combine with the variation in the average chain length in Eq. (4) to determine the overall behavior of the effective exponent $\beta(T)$. For illustration, $\beta(T)$ has been computed (Fig. 3) from the steady-state compliance $J_e g_0 = L\bar{S}_1/(L\bar{S}_2)^2$ using the scission-rodlike model, the activation energies ε_d and ε_s, and the scission energy Δh specified in the caption of Fig. 2. Reported values of Δh for a number of wormlike micellar fluids lie in the range from $20k_BT$ to $70k_BT$, and usually the activation energy ε_d (associated with the rate constant k_d) exceeds the scission energy Δh,[1,40] although independent measurements of each energy are difficult due to the complex interplay between the times scales of chain scission and the diffusive rearrangements and to the impact of the temperature dependence of the average chain length.[41] However, the qualitative behavior of $\beta(T)$ is independent of the specific choice of model parameters.

The most remarkable observation in Fig. 3 is the sigmoidal variation in $\beta(T)$, which is similar to the temperature dependence of the configurational (nonvibrational) entropy of the fluid and of $1-\Phi(T)$ where Φ is the self-assembly order parameter (see inset of Fig. 1 and Ref. 39). A qualitatively similar shape for $\beta(T)$ is found below for the Rouse and reptation models, although the low $\beta \simeq \frac{1}{3}$ plateau emerges independent of L for the rodlike model, while its appearance depends somewhat on L for the Rouse model (see below). The sigmoidal dependence of $\beta(T)$ arises, in part, from the variation in β with the dimensionless parameters r of Eq. (19), which depends on the average chain length, the solvent viscosity (through τ_s^0), the solute concentration, and the temperature. While $\beta(T)$ is a function of these molecular parameters, the qualitative picture of structural relaxation for systems self-assembling on cooling displays the sigmoidal behavior as emerging from the variation with temperature of the ratio of the chain scission time τ_d to the times τ_p of internal cluster motions and the average cluster size L, parameters that shift β in the same direction as does temperature changes.

A similar S-shaped curve is also characteristic of the apparent activation energy E_A computed from the temperature dependence of the terminal relaxation time $\tau_T=\langle\Lambda\rangle$ in an equilibrium associating fluid (as described below). For appreciable scission rates and $\varepsilon_d \gg \Delta h$, the apparent activation energy E_A at intermediate temperatures below T_Φ (i.e., where the solution contains relatively *long* chains that break and recombine *rapidly*) actually exceeds the low temperature limit value of $E_A \simeq \varepsilon_s + (3/2)\Delta h$, corresponding to persistent, almost unbreakable polymers.

This trend for the activation energy of the stress relaxation time parallels the normal trend in glass-forming liquids where E_A increases upon cooling, reflecting the growth of transient polymeric excitation structures below T_Φ.[6,42,43] Consider now self-assembling fluids in the *vicinity* of T_Φ. As the equilibrium chains dissociate into small oligomers and then into the monomers with increasing the temperature, the effective parameters β and E_A describing stress relaxation vary dramatically above T_{sat} even for very slow reaction kinetics ($k_d \simeq 0$), namely, $\beta(T)$ increases from the low plateau level to unity while the apparent activation energy decreases, as is typical for glass-forming fluids. Analytical estimates of this behavior are possible for unbreakable chains ($k_d \simeq 0$). Using the exact discrete chain length distribution, the low frequency limit of the complex modulus yields expressions analogous to Eq. (17) with

$$L\bar{S}_1 = \sum_{N=1}^{\infty} N^3(1-q)q^{N-1} = \frac{1+4q+q^2}{(1-q)^3},$$

$$L\bar{S}_2 = \sum_{N=1}^{\infty} N^6(1-q)q^{N-1} = \frac{1+57q+302q^2+302q^3+57q^3+q^5}{(1-q)^6}. \tag{20}$$

The low temperature $T < T_{\text{sat}}(q \simeq 1)$ steady-state compliance $J_e g_0 \simeq 20$ exactly equals that computed with the continuous distribution ($L \gg 1$) and implies a low β. On the other hand, at high temperatures $T > T_{\text{onset}}(q \simeq 0, L \simeq 1)$, the "shape index" $J_e g_0$ becomes $J_e g_0 \simeq 1$, as expected for the single exponential relaxation limit ($\beta \simeq 1$).

Unlike the impact of reversible reaction kinetics on stress relaxation, the trend in $\beta(T)$ described above is associated with the polymerization transition and reflects the cooperative influence of both polydispersity and scission energy on chain dynamics. Figure 4 depicts the dependence of the computed terminal relaxation time τ_T for almost unbreakable rods (a polydisperse system with $k_d \simeq 0$) over a wide range of temperatures. The stretching exponent $\beta(T) \simeq 0.3$ varies only slightly with temperature for $T < T_\Phi$ but changes dramatically above T_Φ, approaching unity at "high" temperatures $T > T_x$. However, the apparent β derived above T_Φ from $J_e g_0$ describes the low frequency limit of $G^*(\omega)$ rather than $G(t)$. We observe a change in the slope $\beta_t = d\log[-\log[G(t)/G_0]]/d\log t$ for the intermediate time regime where $G(t)/G_0$ relaxes from 0.5 to 0.001. The $\beta(T)$ from fits above T_Φ to the low frequency part $G^*(\omega)/G_0$ increases over an appreciable temperature range, but the average chain length L varies over a limited range, $\Delta L \simeq 1$.

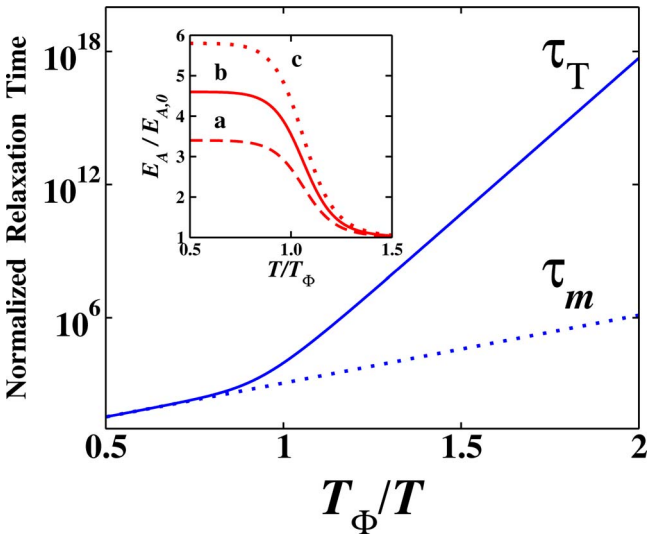

FIG. 4. (Color online) The temperature dependencies of the terminal relaxation time $\tau_T=\langle\Lambda\rangle$ for the rodlike model of unbreakable equilibrium polymers and the relaxation time of the monomers τ_m (both normalized to τ_m^0) as a function of the inverse reduced temperature T_Φ/T. The segmental τ_s and monomer τ_m relaxation times are set equal. The model parameters for the scission energy Δh and activation energies are the same as in Fig. 2. The inset displays the apparent activation energy $E_A = d\log\tau_T/d(1/T)$ divided by the high temperature value $E_{A,0}=\varepsilon_s=8k_BT$ as a function of the reduced temperature T/T_Φ for different scission energies Δh: (a) $13.3k_BT_0$, (b) $20.0k_BT_0$, and (c) $26.7k_BT_0$.

The inset to Fig. 4 shows that the apparent activation energy progressively increases upon cooling. The inset also exhibits the influence of the scission energy on the effective $E_A(T)$. The increase in $E_A(T)$ correlates with the variation in the enthalpy Δh of the assembly process ("sticking energy"). Evidently, decreasing the scission energy (see caption of Fig. 4 for energetic parameters) makes the structural relaxation process more Arrhenius. Thus, both the emergence of dynamic clusters and their persistence in time contribute to the strength of the non-Arrhenius temperature dependence of the structural relaxation time of complex fluids. The temperature dependence of the terminal relaxation time τ_T for an equilibrium mixture of clusters and that for the monomers τ_m merge for $T > T_x$, as demonstrated in Fig. 4. Notice that τ_T grows astronomically in this illustrative example, so that the fluid effectively becomes a solid at some point, a phenomenon recently indicated in certain wormlike micelle solutions.[44]

The relaxation time ratio $\Theta(T)=\tau_T/\tau_s=L\bar{S}_1$ is found to be a universal function of the inverse reduced temperature T_Φ/T for unbreakable rods, yielding a single curve *independent* of Δh but influenced by the chain scission entropy Δs and the total monomer density ϕ. For $T > T_x$, the ratio becomes $\Theta \simeq 1$, while for $T \ll T_\Phi$, $\log\Theta(T)$ becomes linear with slope $\alpha_0(\Delta s, \phi) = d\log\Theta(T)/d(T_\Phi/T)$. Indeed, the polymerization temperature and the scission energy in the FA model are related by $T_\Phi = \delta^{-1}(\Delta s, \phi)\Delta h$, where $\delta(\Delta s, \phi)$ is a factor depending on concentration and entropy of assembly. For low temperatures, $\Theta(T)=6L^3$ and the slope α_0 is deduced as $\alpha_0 = 3\delta(\Delta s, \phi)/2k_B$.

B. Rouse model for equilibrium polymers

Multistep relaxation processes are now described for the Rouse-scission model in a fashion similar to that for the rodlike chain model. The short time behavior again is generally characteristic of the relaxation of monomers and solvent particles, while the long time relaxation is expected to exhibit Rouse-like dynamics for the equilibrium self-assembling fluids. The long time Rouse relaxation process becomes modified by the reversible scission-association events. A multistep relaxation appears in the equilibrium associating Rouse system if the relaxation time $\tau_{N-1} \simeq \tau_0$ of the fastest relaxation mode is comparable to the local monomer/solvent relaxation time τ_m. The ratio τ_0/τ_m depends only on temperature, which therefore acts as a tunable parameter controlling the occurrence of multistep decay in living Rouse systems.

1. Effect of internal chain modes on relaxation

Our previous work formulates a minimal model of viscoelastic and dielectric relaxation in order to explore systematically how the coupling between the scission/association processes and the internal chain rearrangements modifies the relaxation dynamics from that of a frozen polydisperse solution of Rouse chains. The low frequency limit of the complex modulus $G^*(\omega)$ for an equilibrium population of dynamically associating chains is generally[10]

$$G'(\omega)/G_0 = \kappa^2\omega^2\bar{S}_2,$$
$$G''(\omega)/G_0 = \kappa\omega\bar{S}_1, \tag{21}$$

where $G_0=\rho RT/M_0$ is the plateau modulus, $\kappa=(\pi^2/8)\tau_0$, the Rouse constant τ_0 is

$$\tau_0 = \frac{\zeta_0 b^2}{3\pi^2 k_B T}, \tag{22}$$

$\rho=\phi M_0/N_A$ is the mass concentration of the clusters in the solution, ζ_0 is the monomeric friction coefficient, and b is the effective length of a segment. The coefficients $\bar{S}_j$ are computed as the averages over the equilibrium cluster distribution $\bar{S}_j=\Sigma_N L^{-2}Nq^{N-1}S_j$. The quantities $S_j(j=1,2)$ involve sums of contributions from modes with different relaxation times,

$$S_1 = \frac{1}{N}\sum_{p=1}^{N-1}\frac{1}{\sin^2\left(\frac{\pi p}{2N}\right)+a},$$
$$S_2 = \frac{1}{N}\sum_{p=1}^{N-1}\frac{1}{\left(\sin^2\left(\frac{\pi p}{2N}\right)+a\right)^2}, \tag{23}$$

where the dimensionless parameter a depends on the mechanism of the scission/aggregation kinetics,[10]

$$a \equiv \begin{cases} 2\kappa k_d & \text{for MM kinetics} \\ \kappa k_d(2L+N) & \text{for SR kinetics.} \end{cases} \tag{24}$$

The summations in Eq. (23) may be accomplished analytically by contour integration for the scission-Rouse model,[10]

$$S_1 = \frac{\coth x}{\sqrt{a}\sqrt{1+a}} - \frac{1}{2N}\left(\frac{1}{a}+\frac{1}{1+a}\right), \tag{25}$$

$$S_2 = \frac{(1+2a)\coth x}{2\sqrt{a^3}\sqrt{(1+a)^3}} - \frac{N(1-\coth^2 x)}{a(1+a)} - \frac{1}{2N}\left(\frac{1}{a^2}+\frac{1}{(1+a)^2}\right). \tag{26}$$

where

$$x = 2N\,\mathrm{arcsinh}\sqrt{a}. \tag{27}$$

A monodisperse system of frozen nonreacting Rouse chains in solution corresponds to $a=0$, whereupon the sums in Eq. (23) yield

$$S_1 = \frac{2N^2-2}{3N} \simeq \frac{2}{3}N,$$
$$S_2 = \frac{8N^4+20N^2-28}{45N} \simeq \frac{8}{45}N^3. \tag{28}$$

The average over an exponential chain length distribution for a polydisperse system of frozen chains may be evaluated analytically $(j=1,2)$ using the continuous distribution

$$\bar{S}_j = \int_0^\infty \frac{NS_j}{L^2}\exp(-N/L)dN. \tag{29}$$

In particular, for the frozen chain Rouse model with $a=0$, the integrals yield

$$\bar{S}_1 = \tfrac{4}{3}L,$$
$$\bar{S}_2 = \tfrac{64}{15}L^3 \quad (a=0). \tag{30}$$

The opposite limit of reacting chains with rapid reaction processes $(a \gg 1)$ produces

$$S_1 = \frac{1}{a},$$
$$S_2 = \frac{1}{a^2} \quad (a \gg 1). \tag{31}$$

Averaging Eq. (31) over the equilibrium chain length distribution leads to $\bar{S}_j=q_jS_j(L)$ where q_j is independent of L, with $q_1=0.83$ and $q_2=0.76$ for SR kinetics and where $q_1=q_2=1$ for the MM mechanism. The scission rate is inversely proportional to N for the former model, while the latter model has the rates independent of N as in Eq. (24).

We now compare Eq. (11) for the frequency domain transform of the SE function $\mu(t)\equiv\exp[-(t/\tau)^\beta]$ with Eq. (21) for the *normalized* complex modulus $G^*(\omega)/G_0$, where the constant $G_0\equiv G'(\omega\to\infty)$ is chosen as the high frequency

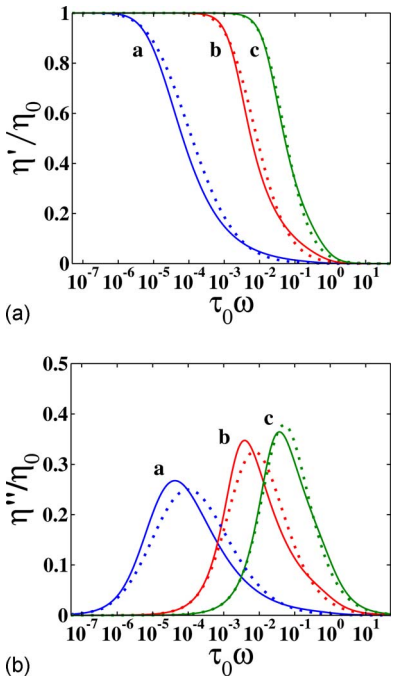

FIG. 5. (Color online) Normalized dynamic viscosity $\eta^*(\omega)=G^*(\omega)/i\omega$ for self-assembling systems with average chain length $L=100$ as a function of the dimensionless frequency $\tau_0\omega$. The solid lines correspond (a) to unbreakable Rouse chains and to living polymers with MM reactions with (b) $\tau_0 k_d=10^{-3}$ and (c) $\tau_0 k_d=10^{-2}$. The dotted lines are their SE fits, which yield (a) $\beta=0.18$, (b) $\beta=0.33$, and (c) $\beta=0.48$. The normalizing coefficients are $\eta_0=CG_0\tau_0$, where C equals (a) 164.5, (b) 22.5, and (c) 7.51. Real components of the shear viscosity η' are displayed in (a), while imaginary components η'' are presented in (b).

limit of the real part of $G^*(\omega)$ in order to generate equations for the β and τ that best approximate the low frequency portion of $G^*(\omega)/G_0$,

$$\frac{\bar{S}_2}{\bar{S}_1^2}=\frac{\beta\Gamma(2/\beta)}{\Gamma^2(1/\beta)}, \tag{32}$$

$$\frac{\tau}{\kappa}=\frac{\bar{S}_2\Gamma(1/\beta)}{\bar{S}_1\Gamma(2/\beta)}. \tag{33}$$

When $a\gg 1$, the reaction kinetics are fast compared to the Rouse relaxation times, and the ratio in Eq. (32) becomes $\bar{S}_2/\bar{S}_1^2\simeq 1$. Hence, the resulting $\beta\simeq 1$ corresponds to an exponential relaxation, with the relaxation time $\tau\simeq\kappa a^{-1}$. On the other hand, when reaction rates are slow, $a\ll 1$, the exponent is $\beta<1$, the effective relaxation time is $\tau\simeq\kappa L^2(16\Gamma(1/\beta)/5\Gamma(2/\beta))$, and β is small for high average chain lengths ($L\gg 1$). Figure 5 depicts the viscoelastic relaxation $\eta^*(\omega)=G^*(\omega)/i\omega$ over the full frequency domain for the Rouse model with several reaction rates, along with the SE fits using parameters evaluated from the low frequency limiting expressions in Eqs. (11), (32), and (33). Although the fits are only to the low frequency region, the correct behavior is well represented over a wide frequency domain apart from the shift in the frequency maximum.

The comparison between Eqs. (32) and (12) enables expressing the dimensionless shape index $J_eG_0=\bar{S}_2/\bar{S}_1^2$ for the stress relaxation function in terms of the coefficients $\bar{S}_j(j=1,2)$. The product J_eG_0 is computed as $0.4N$ for monodisperse frozen Rouse chains, while polydisperse frozen chains (i.e., with infinitely slow chain scissions) have a shape index of $J_eG_0=2.4L$. The stretching exponent computed from Eq. (32), i.e., using the steady-state compliance, equals $\beta\simeq 0.24$ for monodisperse frozen Rouse chains with $N=100$, while the polydisperse frozen system with $L=100$ produces $\beta\simeq 0.18$ from the fit. The steady-state compliance J_e for the scission-Rouse model depends on L when the reaction kinetics are slow (see the frozen chains example above where J_e scales as L), while for faster reaction rates the compliance weakly depends on L, yielding $J_eG_0\simeq 1$ for the fast scission limit. When the parameter $a>0$ is constant as for MM kinetics, β is found to be practically independent of L (for $\beta\geq 0.3$). This comparison demonstrates again that the product $J_eG_0\geq 1$ defines the extent to which the relaxation process of a complex fluid departs from a simple exponential.

2. Single mode approximation

Douglas and Hubbard[15] used the single terminal (longest) mode approximation to analyze the time dependence of $G(t)$ for the Rouse model. Thus, they approximated the Rouse stress relaxation function for monodisperse systems at long times $t>\tau_R$ (as well as the relaxation function for stiff chains) by a single exponential relaxation,

$$G_1(t)/G_0\simeq\frac{1}{N}\exp(-t/\tau_R), \tag{34}$$

where τ_R for the $p=1$ Rouse mode is $\tau_R\simeq\tau_0N^2$. While this mathematical simplification leads to modest errors in the proportionality constants, the scaling laws for viscoelastic and transport properties remain unchanged, as is demonstrated explicitly.

Use of the terminal mode approximation $G(t)$ for the relaxation of associating systems again enables calculation of the apparent β from the low frequency portion of $G_1^*(\omega)/g_{0,N}$, where $g_{0,N}$ is the high frequency limit of the long time approximation to the real part of the complex modulus $g_{0,N}\equiv G'(\omega\gg 0)=G_0/N$. This approximation yields $J_eg_{0,N}=1$ which automatically translates for monodisperse chains to the single mode approximation $\beta=1$, as expected. When the SE is matched using Eqs. (32) and (33) for the Rouse model [see also Eq. (12)] and all modes are retained, the stretched exponent β describes the shape of $G(t)$ quite well in the intermediate time range (Fig. 6) as well as in the long time limit where the fit within the single mode approximation is made. While the longest mode approximation for times $t>\tau_R$ yields a single exponential ($\beta\simeq 1$) for a monodisperse system, polydispersity shifts β to a lower value for an exponential size distribution.

The normalization coefficient g_0 of the single mode approximation [Eq. (34)] for polydisperse systems is the average plateau modulus

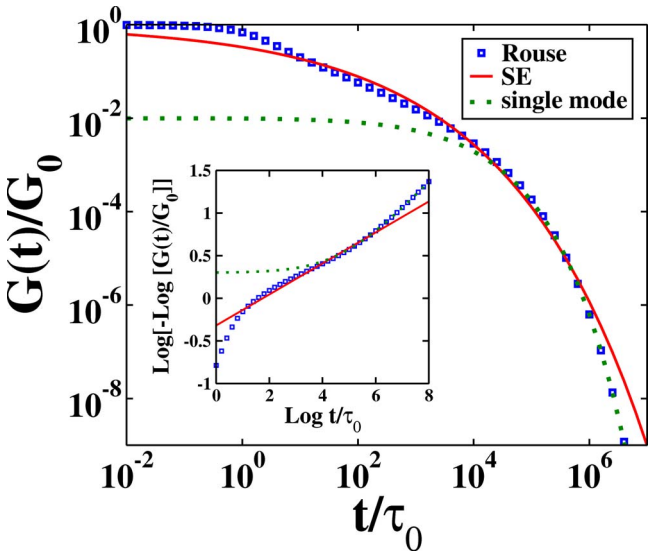

FIG. 6. (Color online) Stress relaxation modulus of unbreakable polydisperse Rouse chains with average chain length $L=100$ (open circles), its SE fit with $\beta=0.18$ obtained from the steady-state compliance J_eG_0 (solid line), and the single $p=1$ mode approximation (dotted line). The inset displays the same curves on different scales but with the same line legends.

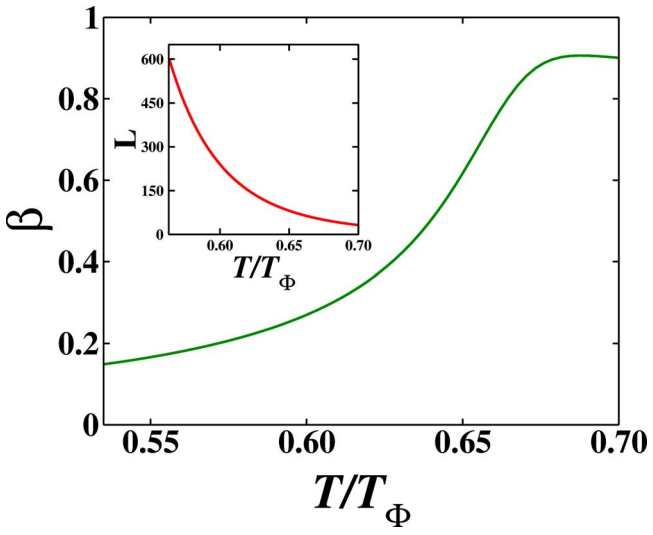

FIG. 7. (Color online) The sigmoidal temperature dependence of the fits of β to the low frequency portion of $G^*(\omega)$ for the scission-Rouse model. The inset presents the temperature dependence of the average chain length. The model parameters are $\Delta h=20k_BT_0$ and $\varepsilon_d-\varepsilon_s=60k_BT_0$. The polymerization temperature T_Φ is determined from the inflection point of $\Phi(T)$ as $T_\Phi=355$ K.

$$g_0=\int_0^\infty \frac{g_{0,N}N}{L^2}\exp(-N/L)dN=\frac{G_0}{L}. \tag{35}$$

Thus, the low frequency behavior of the normalized complex modulus is obtained from Eq. (21), keeping only the $p=1$ mode, and Eq. (35) is

$$G_1'(\omega)/g_0=6\tau_0^2L^4\omega^2,$$
$$G_1''(\omega)/g_0=\tau_0L^2\omega, \tag{36}$$

which gives $J_eg_0=6$ and $\beta\simeq0.38$.

A log-log plot of $G_1(t)$ versus t for monodisperse or polydisperse Rouse chains demonstrates (inset to Fig. 6) three "stages" of relaxation: Early, $t<\tau_0$ (not discussed here), intermediate, $\tau_0<t<\tau_R$, and long time relaxation regimes, $t>\tau_R$. The inset demonstrates that the single mode approximation of Douglas and Hubbard[15] is reasonable for the long time dynamics. While our matching approach analyzes $G^*(\omega)$ and does not apply directly to $G(t)$, the parameters β and τ obtained from low frequency fits to $G^*(\omega)/G_0$ with all modes retained agree well with the computed $G(t)/G_0$ function for the Rouse model in the intermediate time range $k_1\tau_0<t<k_2\tau_R$. The relaxation parameter $\beta\simeq0.38$ derived from $G_1^*(\omega)/g_0$ is more consistent with the $\beta\simeq0.30$ evaluated from time domain calculations of $G_1(t)$ at long times (see Fig. 6). These values are compared to the exact asymptotic value of $\frac{1}{3}$ derived by Douglas and Hubbard[15] based on a steepest descent calculation. The calculated exponent at low temperatures, $\beta\simeq0.30$, is independent of the average chain length, an independence that reflects the averaging over the polydisperse polymer chains. Thus, our approach of using the $n=1$ and $n=2$ moments of the relaxation time distribution probes the shape of the relaxation function on a time scale that overlaps with the relaxation spectrum of the system, while β derived from J_eg_0 of the single mode approximation still yields reasonable agreement with the full $G(t)$ at long times.

Figure 6 compares $G(t)$ for a polydisperse Rouse system with the low frequency SE fit and with $G_1(t)$. The slowest mode approximation is excellent in the long time limit $t>\tau_R$, and this portion of $G(t)$ is well described by the SE model with $\beta\simeq0.30$ (not shown). A linear regime for the Rouse chains is present in the inset at intermediate times. For instance, the relaxation function $G(t)$ for the frozen mixture with $L=100$ is compared with its SE fit with $\beta\simeq0.18$ computed from the steady-state compliance J_eG_0 (as exhibited in the inset), which in the long time limit $\tau>k_2\tau_R$ is followed by another linear regime with $\beta\simeq0.30$ that is obtained for all L in the terminal mode approximation.

The temperature dependence of $\beta(T)$ for the Rouse-scission model is illustrated similarly to that for the rodlike case. The Rouse constant τ_0 is proportional to the monomer friction coefficient, which often follows an Arrhenius behavior in simple fluids,[17]

$$\tau_0=\tau_0^0\exp(\varepsilon_s/T). \tag{37}$$

The variation in $\beta(T)$ has also been computed (Fig. 7) from the steady-state compliance $J_eG_0=\bar{S}_1/\bar{S}_2^2$ using the activation energies ε_d in Eq. (5) and E_r from Eq. (37). The temperature dependence of the average chain length $L(T)$ for the FA model in Eq. (4) requires a specification of the scission energy as Δh. The sigmoidal dependence of β on T arises from the variation with temperature of the dimensionless ratio a of Eq. (24). The contributions from the internal modes makes the small β "plateau" depend on L at low temperatures (where β drops below $\frac{1}{3}$ for flexible chains due to the impact of the internal modes on the relaxation process).

C. Reptation model for equilibrium polymers

Mathematically, the dynamics of the reptation model are analogous to those of the rodlike system since both models de-emphasize the higher $p>1$ modes by the prefactors $1/p^2$ (reptation), or these modes are absent (rodlike), while the structural relaxation times $\tau_{\mathrm{rep},N}$ and $\tau_{\mathrm{rod},N}$ both vary nearly as N^3, and the equilibrium cluster size distributions are specified as identical. Consider first the contribution to the relaxation modulus from chain clustering. Application of Eq. (A33) of Ref. 10 for small ω to the frozen chain reptating system produces the leading term for the modulus of a monodisperse system as,

$$G'(\omega)/G_0 = (\pi^4/120)\tau_{\mathrm{rep},N}^2\omega^2,$$
$$G''(\omega)/G_0 = (\pi^2/12)\tau_{\mathrm{rep},N}\omega, \tag{38}$$

where the plateau modulus G_0 depends on molecular parameters, concentration, and temperature but not on chain length, and the reptation time $\tau_{\mathrm{rep},N}$ is proportional to N^3. A polydisperse frozen system with an exponential chain length distribution merely yields a modification of the constant factors in Eq. (38),

$$G'(\omega)/G_0 = 42\pi^4\tau_{\mathrm{rep}}^2\omega^2,$$
$$G''(\omega)/G_0 = 2\pi^2\tau_{\mathrm{rep}}\omega, \tag{39}$$

where τ_{rep} is the relaxation time for monodisperse chains with length L equal to the average for the polydisperse distribution. Our theoretical prediction of $\beta\simeq 0.33$ for polydisperse frozen chains undergoing reptation dynamics emerges as *independent* of L. An analysis of the Cole–Cole plot of $G'(\omega)$ versus $G''(\omega)$ indicates that the SE fit is reliable not only at low ω but over the full frequency range. Incorporation of "breathing" modes[45] into the reptation model would alter this conclusion, however, leading to a power law intermediate time decay that is qualitatively similar to the flexible chain model described in Sec. II B 2.

The low frequency regime for a living chain system is described by the leading behavior,

$$G'(\omega)/G_0 = \tau_{\mathrm{rep},N}^2\omega^2\bar{S}_2,$$
$$G''(\omega)/G_0 = \tau_{\mathrm{rep},N}\omega\bar{S}_1, \tag{40}$$

with

$$S_1 = \frac{1}{b} - \frac{2\tanh\left(\frac{\pi\sqrt{b}}{2}\right)}{\pi\sqrt{b^3}}, \tag{41}$$

$$S_2 = \frac{1}{2b^2}\left(3 - \tanh^2\left(\frac{\pi\sqrt{b}}{2}\right)\right) - \frac{3\tanh\left(\frac{\pi\sqrt{b}}{2}\right)}{\pi\sqrt{b^5}}, \tag{42}$$

where

TABLE I. SE parameters for monodisperse and polydisperse systems with relatively slow and rapid reaction kinetics.

Model	Type	S_2/S_1^2	β	$\bar{S}_2/\bar{S}_1^2$	β
Rodlike	Frozen	1.0	1.0	20.0	0.28
Reptation	Frozen	1.20	0.85	10.5	0.33
Rouse	Frozen	$0.4N$	[a]	$2.4L$	[a]
Rouse, s.m.[b]	Frozen	1.0	1.0	6.0	0.38
Rapid	MM			1.0	1.0
Rapid	SR			1.1	0.92

[a] $S_2/S_1^2=\beta\Gamma(2/\beta)/\Gamma^2(1/\beta)$.
[b] s.m. means single mode approximation.

$$b \equiv \begin{cases} 2\tau_{\mathrm{rep},N}k_d & \text{for MM kinetics} \\ \tau_{\mathrm{rep},N}k_d(2L+N) & \text{for SR kinetics.} \end{cases} \tag{43}$$

Calculations for frozen chains ($b=0$) yield averaged sums with rather large coefficients $\bar{S}_1=24S_1(L)$, $\bar{S}_2=5040S_2(L)$ [see Eqs. (38) and (39)] compared to the near unity coefficients for highly "dynamic" chains ($b\gg 1$). For example, b large produces $\bar{S}_j=q_jS_j(L)$ with $q_1=0.83$ and $q_2=0.76$ for SR kinetics ($\beta\simeq 0.92$) and $q_1=q_2=1$ for MM kinetics ($\beta=1$). Hence, if $b\gg 1$, the sums satisfy $\bar{S}_1^2\simeq\bar{S}_2\simeq 1/b^2$, and the physical model of rapidly exchanging chains is reflected by $\beta\simeq 1$, i.e., by a nearly single exponential. Thus, analogous to Eq. (32), the SE function provides a similar fit to the scission-reptation model in the low frequency regime, and the exponent β and the relaxation time τ may be found easily from Eqs. (32) and (33) by substituting τ_{rep} for κ by introducing the sums S_j from Eqs. (41) and (42) and by averaging these with Eq. (29).

The shape index J_eG_0 for frozen monodisperse chains is identical to that from a computation of the steady-state compliance.[18] The reptation model for monodisperse polymeric fluids predicts $J_eG_0=1.2$ and $\beta\simeq 0.85$, which corresponds to a nearly exponential relaxation. Polydispersity in the frozen system widens the relaxation time distribution considerably, and hence, the shape index becomes $J_eG_0=10.5$, with $\beta\simeq 0.33$ as found earlier. The latter estimate $\beta\simeq 0.33$ differs somewhat from Cates' proposed value of $\beta\simeq 0.25$ because Cates[29] approximated $\tau\simeq\tau_{\mathrm{rep}}$ in the SE function. Using the same approximation as Cates and matching to the terminal relaxation times for polydisperse chains yield $\langle\Lambda\rangle=\tau\Gamma(1/\beta)/\beta=2\pi^2\tau_{\mathrm{rep}}$, which in turn implies $\beta\simeq 0.26$, in accord with Cates. The steepest descent estimate of Douglas and Hubbard[15] ($\beta\simeq\frac{1}{3}$) from the simple single mode approximation also provides a reasonable approximation for self-assembling fluids with reptation dynamics.

Table I summarizes the calculations of the stretching exponents β along with the parameters $J_eG_0=S_2/S_1^2$ for different dynamical models. Two limiting cases are presented, frozen ($a=0$) chain systems and rapidly reacting ($a\geq 1$) ones. The first two numerical columns correspond to monodisperse (N) chain length distributions, while the last two are for polydisperse exponential distributions whose average length is L.

III. DIELECTRIC RELAXATION IN THE EQUILIBRIUM POLYMER MODELS

The complex permittivity of an associating fluid is now illustrated using the scission-Rouse model[10] in a manner analogous to that for the complex modulus. The low frequency limit of $\epsilon^*(\omega)$ varies as

$$\epsilon'(\omega) = \frac{\epsilon'(\omega) - \epsilon_\infty}{\epsilon_0 - \epsilon_\infty} = 1 - 4\kappa^2\omega^2 S_{2,e},$$
$$\epsilon''(\omega) = \frac{\epsilon'' - \epsilon_\infty}{\epsilon_0 - \epsilon_\infty} = 2\kappa\omega S_{1,e}, \tag{44}$$

where $\epsilon'(\omega)$ and $\epsilon''(\omega)$ are the real and imaginary parts of the normalized dielectric permittivity, and ϵ_0 and ϵ_∞ are the limiting low and high frequency dielectric permittivities. The coefficients $S_{1,e}$ and $S_{1,e}$ are determined from the leading terms of expansions in powers of frequency as

$$S_{1,e} = \sum_{p=1}^{N-1} \frac{1}{p^2\left(\sin^2\left(\frac{\pi p}{2N}\right) + a_e\right)} \quad (p \text{ odd}),$$
$$S_{2,e} = \sum_{p=1}^{N-1} \frac{1}{p^2\left(\sin^2\left(\frac{\pi p}{2N}\right) + a_e\right)^2} (p \text{ odd}). \tag{45}$$

The p^{-2} factor precludes their analytical evaluation of the sums in Eq. (45), but they may be evaluated by contour integration to good accuracy since a previous approximation[10] introduces minimal error (as low as 4% relative error for $N=10$) for low frequencies and long chains,

$$S_{1,e} \simeq \frac{1}{a_e} - \frac{\tanh Ny}{\sqrt{a_e}\sqrt{1+a_e}Ny^2}, \tag{46}$$

$$S_{2,e} \simeq \frac{1}{a_e^2} - \frac{\sqrt{a_e}\sqrt{1+a_e}(2\tanh Ny + Ny\tanh^2 Ny - Ny) + (1+2a_e)y\tanh Ny}{2\sqrt{a_e^3}\sqrt{(1+a_e)^3}Ny^3}, \tag{47}$$

$$y = \operatorname{arcsinh}\sqrt{a_e}, \tag{48}$$

$$a_e = 2a. \tag{49}$$

The contribution to the dielectric permittivity $\epsilon^*(\omega)$ from solutions of chains with length N is determined by the imaginary Laplace transform of the normalized autocorrelation function $\psi_N(t)$ for the chain end-to-end vector.[46] An averaging over the equilibrium chain distribution leads to the dielectric permittivity

$$\epsilon^*(\omega) = \int_0^\infty e^{-i\omega t}\left(-\frac{d}{dt}\psi(t)\right)dt$$
$$= \psi(0) - i\omega\int_0^\infty e^{-i\omega t}\psi(t)dt = 1 - \psi^*(\omega), \tag{50}$$

with $\psi(t) = \Sigma_N L^{-2} N q^{N-1}\psi_N(t)$ being the averaged autocorrelation function. The polydispersity averaged function $\psi(t)$ is fitted again by a SE but perhaps with different parameters β and τ. Then, calculations of $\epsilon^*(\omega)$ in Eq. (50) are compared below with the approximation in which $\psi(t)$ is replaced by a SE function $\mu(t)$. Using Eqs. (11) and (50) the approximate SE model yields the dielectric permittivity at low frequencies ω as

$$\epsilon^*(\omega) = \epsilon'(\omega) - i\epsilon''(\omega)$$
$$\simeq 1 - \frac{1}{\beta}[\Gamma(1/\beta)i\tau\omega + \Gamma(2/\beta)\tau^2\omega^2]. \tag{51}$$

Comparing the approximate $\epsilon^*(\omega)$ from Eq. (51) with Eq. (44) for the scission-Rouse model enables determination of the optimal β and τ. This procedure reproduces Eqs. (32) and (33) but with different coefficients $S_{j,e} \neq S_j (j=1,2)$. Williams and Watts[47] derived the series expansion in Eq. (A3) of $\epsilon^*(\omega)$ for a SE form. However, the alternative series expansion in Eq. (A4) is much more reliable for very small frequencies ω (see the Appendix).

Equations (46) and (47) for frozen Rouse chains ($a=0$) reduce to

$$S_{1,e} \simeq \frac{N^2+1}{3} \simeq \frac{1}{3}N^2,$$
$$S_{2,e} \simeq \frac{6N^4 + 10N^2 + 11}{45} \simeq \frac{2}{15}N^4 \quad (a=0), \tag{52}$$

while averaging Eq. (52) over an exponential distribution gives ($j=1,2$)

$$\bar{S}_1 = 2L^2,$$
$$\bar{S}_2 = 16L^4 \quad (a=0). \tag{53}$$

The dielectric relaxation shape index β for frozen chains is independent of the chain length L because of the scaling of the coefficients $S_{j,e}$ and S_j of Eq. (30) with L. Thus, β emerges from the fit as $\beta=0.45$ for polydisperse solutions of

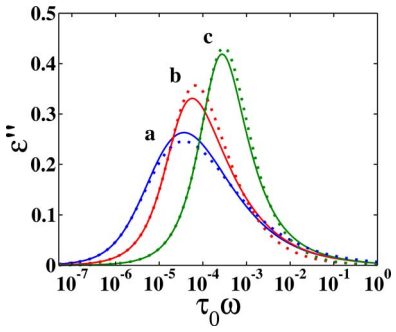

FIG. 8. (Color online) Normalized dielectric loss ϵ'' as a function of dimensionless frequency $\tau_0\omega$ for equilibrium populations of chains with the same average chain lengths $L=100$ and different relaxation dynamics. The solid lines are for (a) unbreakable Rouse chains and living polymers that follow MM reaction kinetics with (b) $\tau_0 k_d=10^{-5}$ and (c) $\tau_0 k_d=10^{-4}$. The dotted lines are the SE fits with (a) $\beta=0.45$, (b) $\beta=0.67$, and (c) $\beta=0.84$.

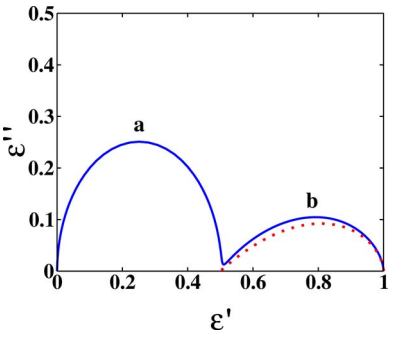

FIG. 9. (Color online) Normalized Cole–Cole plot for polydisperse mixture of unbreakable chains undergoing reptation dynamics at $T \ll T_\Phi$. The multistep dielectric relaxation includes (a) the high frequency relaxation $\epsilon_h^*(\omega)$ of solvent and monomer particles and (b) the low frequency contribution $\epsilon_l^*(\omega)$ associated with chain relaxation. The ratio of the relaxation strengths is taken as $\Delta\epsilon_l/\Delta\epsilon_h=1$. The dotted line is the SE fit of the low frequency process with $\beta=0.33$.

frozen Rouse chains ($a=0$). Equilibrium polymers with frequent scission events ($a_e \geq 1$) yield $S_{1,e}^2 \simeq S_{2,e} \simeq 1/a_e^2$, implying the reduction in exponential relaxation ($\beta \simeq 1$). Figure 8 compares the dielectric loss peaks for the scission-Rouse model with the SE approximation which is quite accurate over the full range displayed even though it arises from fitting of the low frequency behavior.

The shape of the low frequency tail of the loss peak for monodisperse systems is quite accurately represented by a single exponential relaxation since the contributions of the higher modes is de-emphasized by the $1/p^2$ weight factors in Eq. (8). The deviation of the dielectric relaxation function for associating fluids from a simple Debye form arises mostly due to polydispersity. Frozen Rouse chains are characterized by a loss maximum at an inverse frequency of $1/\omega_{\max} \simeq 2.7\tau_0 L^2$ [$0.97\tau_0 N^2$ for a monodisperse system (Ref. 48)] that is comparable to the longest relaxation time. As the scission rate increases, the appropriate β approaches unity, and the τ from the SE fit changes from the scaling $\sim L^2$ for the frozen limit to $\sim L^{-k}$, where $k=0$ for MM and $k=1$ for SR kinetics. Also, retaining a constant ratio $\tau_0 k_d$ between the chain scission time and the Rouse constant (i.e., for MM kinetics), the low frequency fit of β is sensitive to the average chain length L. For instance, at $\tau_0 k_d=10^{-6}$, we find $\beta_1 \simeq 0.52$ for $L_1=100$, while $\beta_2 \simeq 0.84$ for $L_2=1000$. The shape of the dielectric loss peak is determined mostly by the $p=1$ modes of those species whose lengths lie in an interval $L \pm \Delta L$ about the average L. The ratio $\tau_1 k_d \simeq 10^{-2}$ applies for "shorter" chains, while for "longer" chains, $\tau_1 k_d \simeq 1$, making the "chemical" relaxation more effective for longer chains and narrowing the width of the relaxation spectrum distribution, i.e., β increases toward unity. When the chains are nearly frozen (or are frozen), β weakly depends (does not depend) on the average chain length, e.g., for the much smaller $\tau_0 k_d=10^{-9}$ and $L_1=100$ and $L_2=1000$ the resulting $\beta_{1,2} \simeq 0.45$ differ by $\delta\beta=0.01$ even though the average chain length varies by a factor of 10.

The dielectric relaxation spectrum may thus be represented over a wide frequency region as the sum of two relaxations in which the high frequency process is attributed to relaxation of solvent and monomers (generating a peak coinciding with that of the pure solvent for dilute enough solutions[49]), while the low frequency peak comes from internal chain relaxation,

$$\epsilon^*(\omega) = \epsilon_h^*(\omega) + \epsilon_l^*(\omega). \tag{54}$$

Analogous to the short time stress relaxation, the high frequency dielectric relaxation is assumed to obey a Maxwell model for the solvent and monomer particles,

$$\epsilon_h^*(\omega) = \frac{\Delta\epsilon_h}{1 + i\omega\tau_m}, \tag{55}$$

while the low frequency contribution in equilibrium self-assembling solutions is described by one of our chain models. At low temperatures $T \ll T_\Phi (L \gg 1)$, we expect the low and high frequency relaxation processes to be well resolved and produce a double arc Cole–Cole plot. For illustration, Fig. 9 displays the computed frequency dependent dielectric permittivity for a polydisperse mixture of persistent chains undergoing reptation dynamics at low temperatures. Generally, the low frequency "chain" contribution to the dielectric relaxation is given by

$$\epsilon_l^*(\omega) = \Delta\epsilon_l \left[1 - \sum_N L^{-2} N q^{N-1} \psi_N^*(\omega) \right], \tag{56}$$

where

$$\psi_N^*(\omega) = \frac{8}{\pi^2} \tau_{\mathrm{rep},N} \sum_{p=1}^{\infty} \frac{1}{p^2(p^2 + b + i\tau_{\mathrm{rep},N}\omega)} \quad (p \text{ odd}). \tag{57}$$

The exact sum in Eq. (57) is evaluated in the Appendix of Ref. 10 [see Eq. (A30)]. When $b=0 (T \ll T_\Phi)$, the low frequency asymptote of $\epsilon_l^*(\omega)$ is fitted by a SE with $\beta \simeq 0.33$ since $\psi(t)=g(t)$ for the reptation model, and hence, the same β and τ emerge from fitting the low frequency dielectric relaxation $\epsilon^*(\omega)$ and stress relaxation $G^*(\omega)/G_0$ functions.

The multistep dielectric relaxation is depicted in Fig. 9 in terms of a normalized Cole–Cole plot. The ratio of the relaxation strengths of the low and high frequency contributions strongly depends on concentration,[49] and the value taken is indicated in the caption. At higher temperatures the

average chain length L decreases, leading to a smoothing and disappearance of the dip. When L is large enough ($\Phi \simeq 1$), the Cole–Cole plot remains unchanged by further lowering of the temperature.

IV. CONCLUSIONS

We study minimal models for the viscoelastic and dielectric relaxations of fluids self-assembling into chainlike clusters that form and disintegrate reversibly at equilibrium. The relaxation dynamics predicted for these fluids using classical polymer dynamic models are largely affected by the competition between the chemical SR and internal chain relaxation processes. The computed steady-state compliances are fitted to SE functions, which are often used to analyze experimental data. The relaxation modulus $G(t)$ calculated for three dynamical models (rodlike, Rouse, and reptation) are well approximated by a SE relaxation over an appreciable time range, a feature often observed experimentally for the long time relaxation of complex fluids. The exponents β deduced from the computed low frequency behavior of $G^*(\omega)$ enable us to describe an intermediate time regime that overlaps with the characteristic relaxation times of the chains. The theory is illustrated in detail for the stress relaxation of rodlike and of Rouse chains with an exponential chain distribution derived from the theory. The long time contribution to $G(t)$ for unbreakable chains behaves as a SE with $\beta \simeq 0.3$ at low temperatures and is thus similar to the relaxation functions for polydisperse systems whose dynamics is effectively described by a single relaxation mode (rodlike macromolecules or reptative chains).

Our model yields a sigmoidal dependence of the stretching exponent β both as a function of the ratio of the scission time to the characteristic time for internal chain motions and temperature. For systems that associate upon cooling, the chain scission time at low temperatures is large compared to the time scale of diffusive rearrangements of the clusters, thereby producing a plateau with small β at low temperatures. On the other hand, the high temperature system is composed of either short oligomers or long chains that decompose and recombine rapidly, and consequently, the stress relaxation approaches another plateau in β with $\beta \simeq 1$ at high temperatures. The transition zone in the stress relaxation from the highly stretched to a nearly exponential regime evolves naturally as temperature increases, and the relaxation spectrum narrows, a phenomenon also exhibited rather generally in the dynamics of glass formation.[50] Unbreakable polymers or simple fluids have an effective relaxation time that is a weak function of temperature, in contrast to associating fluids, living polymers, and micellar solutions where a strong temperature dependence emerges from an increase in the dissociation rate constant k_d as temperature is elevated. We also demonstrate the relationship of the stretching exponent β to the molecular parameters of the chain models.

An additional motivation for investigating the dynamics of equilibrium self-assembly arises from the suggestion by Douglas and Hubbard[15] that the "dynamically heterogeneous" structures forming and disintegrating in dynamical equilibrium in cooled liquids (where crystallization is suppressed) can be understood as a kind of self-assembly. In particular, based on symmetry arguments applied to exact formal integral equations describing relaxation in fluids at equilibrium along with experimental observations for stress relaxation in glass-forming liquids, Douglas and Hubbard[15] hypothesized that these heterogeneities should take the form of *equilibrium polymers*, thereby rationalizing many universal aspects of stress relaxation in glass-forming liquids. Since their work, much evidence from both simulations for glass-forming liquids and direct observations of the dynamics of colloidal fluids has accumulated, supporting their hypothesis (see Ref. 51 for a discussion and for a fit of the temperature dependence of the mass distribution for mobile strings to a self-assembly model of the kind described in the present paper). The phenomenological similarity between the dynamics of associating polymers and the dynamics of glass-forming liquids has been established by Kumar and Douglas[52] and recently by other authors.[53,54] The original work of Douglas and Hubbard[15] models the dynamic heterogeneity of glasses as a kind of equilibrium polymerization, assuming, in effect, that the transient clusters are rigid over the times of the stress relaxation. Thus, the analogy with conventional equilibrium polymers is evident. Mobile particle chains clearly cannot be equated with conventional polymers in terms of their impact on the chain viscoelasticity, although the growing length of the polymers upon cooling certainly correlates with both the increase in the apparent activation energy and the decrease in the configurational entropy in cooled liquids. Simulations[55–57] indicate that both the mobile and immobile particle clusters grow into polymer structures in a complementary fashion upon cooling, so that the presence of one class of clusters seems to imply the other. Given the complexity of the clustering phenomenon occurring in glass-forming liquids, a direct application of our model to this class of complex fluids requires caution. Nonetheless, we expect that the main cause of the multistep relaxation in glass-forming liquids is the presence of polydisperse immobile particle clusters, as originally envisioned by Douglas and Hubbard.[15]

Consistent with this conjectured relationship between self-assembling fluids and glass-forming liquids, a monotonic decrease in β has been reported in both structural glass-forming liquids[2,4–6,8,9,58,59] and even magnetic glass-forming materials.[60] The present theoretical framework for self-association indicates that this variation in β arises from an averaging over a polydisperse chain distributions at equilibrium and a phenomenology that is strikingly reminiscent of the phenomenology of glass-forming liquids. While the original Douglas–Hubbard equilibrium polymerization model of stress relaxation in glass-forming liquids simply assumes that a single chain relaxation mode dominates the relaxation process, the single mode approximation is found here to be good for rodlike chains and chains exhibiting reptative dynamics but only qualitative for flexible associating chains in the long time limit.

As mentioned in Sec. I, both the theoretical arguments of Douglas and Hubbard[15] and the present treatment of associating fluids omit hydrodynamic interactions associated with collective momentum diffusion in the fluid. Even in simple fluids,[61] these long range interactions lead to memory effects

in stress relation. Consequently, the velocity autocorrelation function associated with particle diffusion incurs a nonexponential (power law) long time relaxation due to hydrodynamic interactions. These interactions are neglected here because the interest lies in the longer time relaxation where the heterogeneities in the fluid associated with assembled clusters are expected to dominate the fluid relaxation. Our treatment is quite consistent with other treatments of the dynamics of polymer solutions where hydrodynamic interactions are neglected.

The scission-Rouse model of self-assembling polymer solutions is also used to obtain basic qualitative insights into the dielectric relaxation of associating fluids. Our model calculations indicate that the dynamic heterogeneity of the associating fluid produces relaxation that is well described by a SE function, but β and τ are found to differ from the corresponding quantities obtained from modeling stress relaxation. The β and τ estimated from the computed loss peaks are found to be useful for representing the complex permittivity of an associating fluid as a function of temperature, chain length, and concentration. The form of the dielectric loss peak is sensitive to the "efficiency" of the scission dynamics, as governed by the dimensionless parameter a. For fixed and *nonzero* $a>0$, the shape of the dielectric loss peak $\epsilon''(\omega)$ strongly depends on L. Similarly, frozen chains with a near zero yield a loss peak that is insensitive to the chain length, a theoretical observation that may be useful for tracking the dynamics of chains in self-associating solutions and in estimating the reaction rates.

ACKNOWLEDGMENTS

This research is supported, in part, by NSF Grant No. CHE-0749788 and by the Joint Theory Institute which is funded by the University of Chicago and Argonne National Laboratory. We are grateful to Jacek Dudowicz for many helpful discussions.

APPENDIX: STRETCHED EXPONENTIAL AND COLE–DAVIDSON RELAXATION FUNCTIONS

1. Analytical representation of stretched exponential function in the frequency domain

The Laplace transform of the SE function $\mu(t)$ into the frequency domain,

$$\mu^*(\omega,\tau,\beta)=i\omega\int_0^\infty e^{-i\omega t}\mu(t)dt=i\omega\int_0^\infty e^{-i\omega t}e^{-(t/\tau)^\beta}dt \tag{A1}$$

cannot be performed analytically. Thus, we consider tractable representations for the SE function in the frequency domain. This transformation may, however, be developed as a power series expansion in ω. Representing the Laplace–Fourier transform as

$$\mu^*(z,\beta)=iz\int_0^\infty e^{-izt}e^{-t^\beta}dt, \tag{A2}$$

with $z=\omega\tau$ the reduced frequency, alternative power series expansions may be introduced by expanding either of the two exponentials in Eq. (A2). Expanding the first e^{-t^β} term yields the series representation[62]

$$\mu^*(z,\beta)=\sum_{n=0}^{\infty}\frac{1}{z^{n\beta}}\frac{\Gamma(n\beta+1)}{\Gamma(n+1)}\times\left[\sin\frac{\pi}{2}(n\beta+2n+1)+i\cos\frac{\pi}{2}(n\beta+2n+1)\right], \tag{A3}$$

which converges rapidly for large $z=\omega\tau$ but experiences convergence problems when z approaches zero. The alternative expression for $\mu^*(z,\beta)$ is generated by expanding the e^{-izt} term,

$$\mu^*(z,\beta)=\frac{1}{\beta}\sum_{n=0}^{\infty}\frac{z^{n+1}}{n!}\Gamma\left(\frac{n+1}{\beta}\right)\left[\sin\frac{\pi n}{2}+i\cos\frac{\pi n}{2}\right]. \tag{A4}$$

These asymptotic series are summed until the next neglected term in the series begins to increase in absolute value.

Useful checks on numerical approximations are provided by the specific cases of $\beta=0,\frac{1}{2},1$, where the Fourier–Laplace transform can be effected analytically. The optimal point z_{tr} where the two series expansions should be joined is found by minimizing the absolute difference between Eqs. (A3) and (A4) as a function of z and M, where M is the number of terms retained from Eq. (A4) for the asymptotic series at low z. Calculations for z_{tr} and M over a range of parameters β have been approximated using cubic polynomials to describe $\log z_{tr}$ and $\log M$ as functions of $\log\beta$.

2. Cole–Davidson and stretched exponential models: Analytical interrelations

The Havriliak–Negami (HN) equation

$$\phi^*(\omega)=\frac{1}{[1+(i\omega\tau)^\alpha]^\beta} \tag{A5}$$

is often used to model relaxation phenomena,[63] where $\phi^*(\omega)$ is the normalized relaxation function. Davidson and Cole found that an appreciable amount of dielectric relaxation data may be fitted by Eq. (A5) ($\alpha=1$, $0<\beta\leq 1$). The relaxation functions $\phi^*(\omega)$ is related to its time domain counterparts $\phi(t)$ by a transformation as in Eq. (A1). Lindsey and Patterson[64] studied the ability of the CD ($\alpha=1$) to reproduce the Laplace transform of the SE (Ref. 64) and concluded that the CD and SE relaxation function have similar shapes, but their time distribution functions $\rho(\tau)$ are very different at long times.[64] Snyder and Mopsik[65] demonstrated that with achievable instrumental accuracy, the HN and SE relaxation functions are distinguishable. Here we determine the exponents β associated with CD and SE relaxation functions by fitting their moments $\langle\Lambda^n\rangle$,

$$\langle\Lambda^n\rangle=\int_0^\infty\tau^n\rho(\tau)d\tau=\frac{1}{(n-1)!}\int_0^\infty t^{n-1}g(t)dt, \tag{A6}$$

rather than globally comparing their shapes as a function of time or of frequency. Expanding the low frequency portion of the complex modulus and dielectric permittivity as a se-

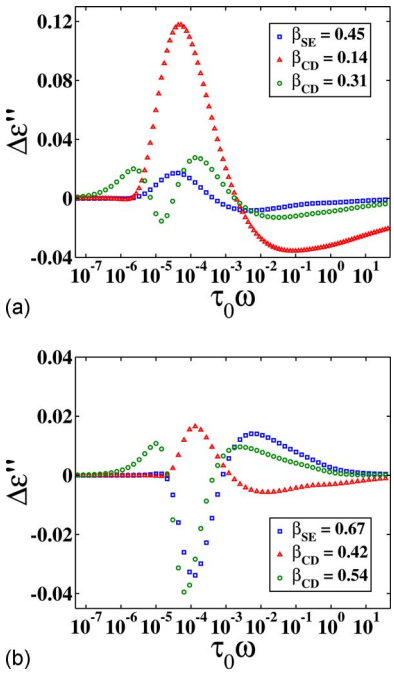

FIG. 10. (Color online) Differences between imaginary parts of the normalized dielectric permittivities in the scission-Rouse and the SE or CD models $\Delta\epsilon''$ as a function of dimensionless frequency $\tau_0\omega$ for equilibrium chain population with equal average chain lengths $L=100$ and different relaxation dynamics: (a) unbreakable Rouse chains and (b) living polymers with MM reaction kinetics and $\tau_0 k_d = 10^{-5}$. The parameters β for each model are presented in the legends. The exponent β_{CD}, which was presented first in (a) and (b), is evaluated analogous to β_{SE}, while the second value β_{CD} in the legends is obtained using the relations of Lindsey and Patterson (Ref. 64).

ries in ω yields the moments $\langle\Lambda^n\rangle$ as the coefficients of those expansions,

$$\langle\Lambda^n\rangle_{SE} = \frac{\tau_{SE}^n}{(n-1)!}\frac{\Gamma(n/\beta_{SE})}{\beta_{SE}}, \tag{A7}$$

$$\langle\Lambda^n\rangle_{CD} = \frac{\tau_{CD}^n}{n!}\prod_{i=1}^{n}(\beta_{CD}+i-1). \tag{A8}$$

Equating the $n=1$ and $n=2$ moments of the SE and CD functions yields the nonlinear interrelations between β and τ for the SE and CD dynamics as

$$\beta_{CD} = \frac{1}{u-1}, \qquad \tau_{CD} = \frac{\tau_{SE}\Gamma(1/\beta_{SE})}{\beta_{SE}\beta_{CD}}, \tag{A9}$$

where $u = 2\beta_{SE}\Gamma(2/\beta_{SE})/\Gamma^2(1/\beta_{SE})$.

As exhibited by Fig. 10, classical Rouse-like behavior for frozen chains is reproduced quite well by the dielectric loss peak from the SE function whose $\beta_{SE}\simeq 0.45$ is evaluated from a fit to the low frequency limit, while the analogous best low frequency CD relaxation function with $\beta_{CD}\simeq 0.14$ does not fit $\epsilon''(\omega)$ near ω_{max}. The parameter $\beta_{CD}\simeq 0.31$, which emerges from a global least-squares fitting,[64] provides a much better description with the CD equation. However, this approximation degrades in accuracy at low frequencies. When chain reactions are present and the exponents are larger, the CD equation with β evaluated from the low frequency behavior better reproduces the dielectric loss peak in the scission-Rouse model, and both SE and CD functions are reliable approximations (see Fig. 10).

[1] M. E. Cates and S. J. Candau, J. Phys.: Condens. Matter **2**, 6869 (1990).
[2] Ch. Simon, G. Faivre, R. Zorn, F. Batallan, and J. F. Legrand, J. Phys. I **2**, 307 (1992).
[3] A. M. Ketner, R. Kumar, T. S. Davies, P. W. Elder, and S. R. Raghavan, J. Am. Chem. Soc. **129**, 1553 (2007).
[4] M. Cutroni, A. Mandanici, A. Spanoudaki, and R. Pelster, J. Chem. Phys. **114**, 7118 (2001).
[5] M. Cutroni and A. Mandanici, J. Chem. Phys. **114**, 7124 (2001).
[6] M. Cutroni, A. Mansanici, and A. Piccolo, J. Phys.: Condens. Matter **7**, 6781 (1995).
[7] R. D. Groot and W. G. M. Agterof, Macromolecules **28**, 6284 (1995).
[8] R. Bohmer and C. A. Angell, Phys. Rev. B **48**, 5857 (1993).
[9] R. Bohmer and C. A. Angell, Phys. Rev. B **45**, 10091 (1992).
[10] E. B. Stukalin and K. F. Freed, J. Chem. Phys. **125**, 184905 (2006).
[11] K. F. Freed and S. F. Edwards, J. Chem. Phys. **61**, 3626 (1974).
[12] E. Leutheusser, Phys. Rev. A **29**, 2765 (1984); C. Z.-W. Liu and I. Oppenheim, Physica A **235**, 369 (1997).
[13] U. Bengtzelius, W. Gotze, and A. Sjolander, J. Phys.: Condens. Matter **17**, 5915 (1984); L. Sjogren, Z. Phys. B: Condens. Matter **79**, 5 (1990).
[14] K. S. Schweizer and E. J. Saltzman, J. Chem. Phys. **119**, 1181 (2003); **121**, 1984 (2004).
[15] J. F. Douglas and J. B. Hubbard, Macromolecules **24**, 3163 (1991).
[16] H. Yamakawa, Macromolecules **8**, 339 (1975).
[17] J. D. Ferry, *Viscoelastic Properties of Polymers*, 3rd ed. (Wiley, New York, 1980).
[18] M. Doi and S. F. Edwards, *The Theory of Polymer Dynamics* (Oxford University Press, New York, 1986).
[19] R. E. Rouse, J. Chem. Phys. **21**, 1272 (1953).
[20] M. Mondello, G. S. Grest, E. B. Webb III, and P. Peczak, J. Chem. Phys. **109**, 798 (1998).
[21] J. Dudowicz, K. F. Freed, and J. F. Douglas, J. Chem. Phys. **119**, 12645 (2003).
[22] A. Milchev, Y. Rouault, and D. P. Landau, Phys. Rev. E **56**, 1946 (1997).
[23] M. S. Turner and M. E. Cates, J. Phys. (France) **51**, 307 (1990).
[24] C. M. Marques, M. S. Turner, and M. E. Cates, J. Chem. Phys. **99**, 7260 (1993).
[25] J. Dudowicz, K. F. Freed, and J. F. Douglas, J. Chem. Phys. **111**, 7116 (1999).
[26] K. Pendyala, X. Gu, K. P. Andrews, K. Gruner, D. T. Jacobs, and S. C. Greer, J. Chem. Phys. **114**, 4312 (2001).
[27] G. Faivre and J. L. Gardissat, Macromolecules **19**, 1988 (1986).
[28] C.-C. Huang, H. Xu, and J.-P. Ryckaert, J. Chem. Phys. **125**, 094901 (2006).
[29] M. E. Cates, Macromolecules **20**, 2289 (1987).
[30] N. A. Spenley, M. E. Cates, and T. C. B. McLeish, Phys. Rev. Lett. **71**, 939 (1993).
[31] P. Fischer and H. Rehage, Langmuir **13**, 7012 (1997).
[32] H. Rehage and H. Hoffmann, Mol. Phys. **74**, 933 (1991).
[33] B. O'Shaughnessy and J. Yu, Phys. Rev. Lett. **74**, 4329 (1995).
[34] P. Terech, V. Schaffhauser, P. Maldivi, and J. M. Guenet, Langmuir **8**, 2104 (1992).
[35] A. Khatory, F. Lequeux, F. Kern, and S. J. Candau, Langmuir **9**, 1456 (1993).
[36] J. F. A. Soltero, J. E. Puig, and O. Manero, Langmuir **12**, 2654 (1996).
[37] A. Shukla, R. Fuchs, and H. Rehage, Langmuir **22**, 3000 (2006).
[38] M. S. Turner and M. E. Cates, Langmuir **7**, 1590 (1991).
[39] R. Granek and M. E. Cates, J. Chem. Phys. **96**, 4758 (1992).
[40] I. Couillet, T. Hughes, G. Maitland, F. Candau, and S. J. Candau, Langmuir **20**, 9541 (2004).
[41] W. Knobben, N. A. M. Besseling, and M. A. C. Cohen Stuart, J. Chem. Phys. **126**, 024907 (2007).
[42] P. B. Macedo and A. Napolitano, J. Chem. Phys. **49**, 1887 (1968).
[43] M. L. Mansfield, Phys. Rev. E **66**, 016101 (2002).
[44] R. Kumar, G. C. Kalur, L. Ziserman, D. Danino, and S. R. Raghavan, Langmuir **23**, 26 (2007).
[45] R. Granek, Langmuir **10**, 1627 (1994).
[46] N. G. McCrum, B. E. Read, and G. Williams, *Anelastic and Dielectric*

Effects in Polymeric Solids (Wiley, London, 1967).
[47] G. Williams, D. C. Watts, S. B. Dev, and A. M. North, Trans. Faraday Soc. **67**, 1323 (1971).
[48] S. S. Patel and K. M. Takahashi, Macromolecules **25**, 4382 (1992).
[49] N. Miura, N. Shinyashiki, and S. Mashimo, J. Chem. Phys. **97**, 8722 (1992).
[50] J. C. Phillips, Phys. Rev. E **53**, 1732 (1996).
[51] J. F. Douglas, J. Dudowicz, and K. F. Freed, J. Chem. Phys. **125**, 144907 (2006).
[52] R. Kumar and J. F. Douglas, Phys. Rev. Lett. **87**, 188301 (2001).
[53] A. R. C. Baljon, D. Flynn, and D. Krawzsenek, J. Chem. Phys. **126**, 044907 (2007).
[54] P. N. Segre, V. Prasad, A. B. Schofield, and D. A. Weitz, Phys. Rev. Lett. **86**, 6042 (2001).
[55] A. I. Mel'cuk, R. A. Ramos, H. Gould, W. Klein, and R. D. Mountain, Phys. Rev. Lett. **75**, 2522 (1995).
[56] M. Dzugutov, S. I. Simdyankin, and F. H. M. Zetterling, Phys. Rev. Lett. **89**, 195701 (2002).
[57] M. Wilson and P. A. Madden, Mol. Phys. **92**, 197 (1997).
[58] A. Schonhals, F. Kremer, A. Hofmann, E. W. Fischer, and E. Schlosser, Phys. Rev. Lett. **70**, 3459 (1993).
[59] J. N. Roux, J. L. Barrat, and J. P. Hansen, J. Phys.: Condens. Matter **1**, 7171 (1989).
[60] R. V. Chamberlin, J. Appl. Phys. **57**, 3377 (1985).
[61] B. J. Alder, D. M. Gass, and T. E. Wainright, J. Chem. Phys. **53**, 3813 (1970).
[62] R. Ferguson, V. Arrighi, I. J. McEwen, S. Gagliardi, and A. Triolo, J. Macromol. Sci. Part B: Phys. **45**, 1065 (2006).
[63] S. Havriliak, Jr. and S. Negami, J. Polym. Sci., Part C: Polym. Symp. **14**, 99 (1966).
[64] C. P. Lindsey and G. D. Patterson, J. Chem. Phys. **73**, 3348 (1980).
[65] C. R. Snyder and F. I. Mopsik, Phys. Rev. B **60**, 984 (1999).